

# Local Pharmacokinetic Analysis of a Stable Spin Probe in Mice by *In Vivo* L-band ESR with Surface-coil-type Resonators

MASAYUKI KAMATARI<sup>a</sup>, HIROYUKI YASUI<sup>a</sup>, TATEAKI OGATA<sup>b</sup> and HIROMU SAKURAI<sup>b,\*</sup>

<sup>a</sup>Department of Analytical and Bioinorganic Chemistry, Kyoto Pharmaceutical University, 5 Nakauchi-cho, Misasagi, Yamashina-ku, Kyoto 607-8414, Japan; <sup>b</sup>Department of Chemistry and Chemical Engineering, Faculty of Engineering, Yamagata University, 4-9-16 Jyonan, Yonezawa, Yamagata 992-8510, Japan

Accepted by Professor E. Niki

(Received 9 March 2002; In revised form 21 May 2002)

*In vivo* ESR spectroscopy using a low frequency microwave of approximately 1 GHz has been developed to measure non-invasive ESR spectra in animals given paramagnetic compounds, in which a loop-gap-type resonator was used and ESR spectra were measured at the animal's head or abdomen. Therefore, the concentrations of paramagnetic species in both the blood and organs were compositely contributed to the spectra. When we understand the kinetics of paramagnetic species in detail, it is essentially important to know how these kinetics are expressed in each organ. For this purpose, a surface-coil-type resonator, which enabled local ESR measurement in specific organs, has been developed. By using this method, we studied the real-time pharmacokinetics of spin clearance curves detected in the organs of mice given 4-hydroxy-2,2,6,6-tetramethylpiperidine-1-oxyl (4-hydroxy-TEMPO) intravenously (i.v.), by monitoring the inferior vena cava, liver and kidney. Quantified clearance curves in the organs were analyzed on the basis of a two-compartment model, and pharmacokinetic parameters were estimated based on the curve-fitting. The obtained pharmacokinetic parameters were found to depend on the measurement site, and the distribution and elimination processes of the spin probe were successfully separated between the blood and organs of mice.

**Keywords:** Local pharmacokinetics; *In vivo* L-band ESR; Surface-coil-type resonator; Spin probe; Free radical

## INTRODUCTION

*In vivo* measurement of paramagnetic species is needed in order to understand their biochemical and

physiological roles in living animals.<sup>[1–3]</sup> The development of *in vivo* L-band ESR equipped with a loop-gap-type resonator<sup>[4–7]</sup> has made it possible to measure non-invasive ESR<sup>[8,9]</sup> and the imaging<sup>[10,11]</sup> of paramagnetic species in live animals, in spite of involving problems such as relatively low sensitivity. In the conventional *in vivo* ESR using a low frequency microwave of around 1 GHz, ESR spectra were usually observed at the head<sup>[12–15]</sup> or abdomen<sup>[16]</sup> of animals who received stable spin probes. Based on the measurement of the relative clearance rate constants of ESR signal intensities due to the administered spin probes, the reduction ability of the compounds<sup>[15–17]</sup> and the oxidative stress induced by reactive oxygen species (ROS)<sup>[18–20]</sup> were examined in live animals.

Because the detection sensitivity in the L-band ESR equipped with a loop-gap-type resonator has depended on the volume of the measuring objects, it has been difficult to determine the spin concentration in animals. Therefore, in 1999, we proposed a quantitative pharmacokinetic analysis of spin probes by monitoring the head and abdomen of mice by using L-band ESR equipped with a loop-gap-type resonator, in which the spin clearance curves were analyzed with the Michaelis-Menten elimination models and were evaluated in terms of the nonlinear pharmacokinetic parameters contributing to the dose- and age-dependent spin clearance of the spin probes.<sup>[21]</sup> However, the concentrations of spin

\*Corresponding author. Tel.: +81-75-595-4629. Fax: +81-75-595-4753. E-mail: sakurai@mb.kyoto-phu.ac.jp

probes in both the blood and organs compositely contributed to the obtained ESR spectra in combination. In order to understand the pharmacokinetics of the spin probes in detail, we have to know how their pharmacokinetics are expressed in each organ of the animals. The conventional L-band ESR with the loop-gap-type resonator has indeed an advantage in the non-invasive *in vivo* detection of paramagnetic species, however, it is impossible to analyze the local ESR signals of the species existing in specific organs of animals involving the circulating blood.<sup>[22,23]</sup> In order to more precisely examine the pharmacokinetics of spin probes, a new analytical method to detect paramagnetic species in each organ of the animal needs to be established.

For this purpose, surface-coil-type resonators (SCRs) have been proposed for the local L-band ESR measurement,<sup>[24–26]</sup> which were successfully used for detecting the paramagnetic species in several organs of rats and mice<sup>[26–28]</sup> and in leaves of plants.<sup>[29]</sup> In addition, the half-life of 4-hydroxy-2,2,6,6-tetramethylpiperidine-1-oxyl (4-hydroxy-TEMPO) was found to depend on the organs of rats.<sup>[27,28]</sup> However, in that case a precise pharmacokinetic analysis was not performed. Then, by using this minimal invasive method with both flexible and semirigid surface-coil-type resonators for *in vivo* L-band ESR, we studied the quantitative pharmacokinetics of 4-hydroxy-TEMPO in mice. The local disposition of 4-hydroxy-TEMPO was sufficiently evaluated based on the multiple clearance curves of its concentrations in the blood and in organs such as the liver and kidney of mice.

## EXPERIMENTAL

### Materials

4-Hydroxy-TEMPO was purchased from Sigma Chemical Co. (St. Louis, MO, USA), and was used without further purification. This probe was dissolved at appropriate concentrations in physiological saline (0.9% NaCl solution). Nembutal (Sodium pentobarbital: 50 mg/ml) was obtained from Abbot Laboratories Co. (USA). Polyethylene tubes (600  $\mu$ l) were from Quality Scientific Plastics Co. (USA). Other reagents were of the highest purity commercially available.

### Animals

Male std-ddy mice (6 weeks old, 30 g) were purchased from Shimizu Experimental Material Co. (Kyoto, Japan) and maintained on a light/dark cycle in the central animal facility of Kyoto Pharmaceutical University. They were given free access to standard mice chow and water *ad libitum*. All experiments were approved by the Experimental Animal

Research Committee of Kyoto Pharmaceutical University (KPU) and performed according to KPU's Guidelines for Animal Experimentation.

### Flexible and Semirigid Surface-coil-type Resonators (FSCR and SRSCR)

FSCR and SRSCR (SCRs), prepared as described previously,<sup>[24,28]</sup> consisted of a single-turn coil with diameters of 5 and 11 mm, respectively, and a balanced transmission line made of two flexible and semirigid coaxial lines with a 50  $\Omega$  characteristic impedance, respectively. Their single-turn coils were constructed from copper wire of 0.32 and 0.5 mm in diameter, respectively. The length of the transmission line was calculated on the basis of the diameters of the coil and wire as well as on the resonant frequency. SCR were connected to the L-band ESR through a three-stub tuner and driven at a frequency of approximately 1.1 GHz. The coil was aligned in a direction which made the microwave magnetic field generated in the coil perpendicular to the static magnetic field in the same manner as in a usual ESR measurement.

## Methods

### *Animal Experiments and Administration Methods of 4-hydroxy-TEMPO in Mice*

A FSCR of 5 mm in diameter was used for the measurement performed in the mouse's blood vessel of the inferior vena cava (the circulating blood) and tail. A SRSCR of 11 mm in diameter was used for the measurement on the surface of the liver and kidney. Mice were anesthetized by intraperitoneal (i.p.) injection of pentobarbital at a dose of 50 mg/kg body weight. After the abdomen was opened through a middle incision, the FSCR was tied up with the vessel of the inferior vena cava by silk thread for surgery, while the SRSCR was fixed tightly on the surface of the liver or kidney. Then, after the abdomen was sutured, the anesthetized mice with SCR were fixed on a handmade Teflon holder and inserted into the cavity of the L-band ESR. For the measurement in the tail, the tail was passed through the FSCR and fixed at its root without the use of any invasive surgical procedures. The anesthetized mice were then fixed in the same manner as mentioned above.

4-Hydroxy-TEMPO dissolved in saline was intravenously (i.v.) bolus administered into the tail vein by using a needle equipped with a 1 ml syringe, and L-band ESR spectra due to the spin probe were measured immediately after the injection. For ESR measurement in the blood, 4-hydroxy-TEMPO was administered at the doses of 0.13, 0.25, 0.5, 0.75 and 1.0 mmol/kg body weight. For the measurements in

the liver and kidney, the spin probe was administered at the doses of 0.25, 0.5, 0.75 and 1.0 mmol/kg body weight. For the measurements in the tail, the spin probe was administered at the doses of 0.5 and 1.0 mmol/kg body weight.

#### ***In Vivo L-band ESR Measurements with Surface-coil-type Resonators***

ESR spectra of paramagnetic species due to 4-hydroxy-TEMPO were measured at every 30 s using an L-band ESR spectrometer JES-RE-3L (JEOL, Japan) equipped with handmade surface-coil-type resonators (FSCR and SRSCR) and an R3361A Spectrum Analyzer (Advantest, Japan). The cavity of the ESR spectrometer was maintained at a constant temperature (37°C), which was adjusted by water circulating through a thermo-regulated water bath. Instrumental conditions for the L-band ESR measurements were as follows: microwave frequency 1.1 GHz, microwave power 10 mW for all measurements except those with the blood at the dosage of 0.13 mmol/kg, in which microwave power was 30 mW, modulation frequency 100 kHz, modulation amplitude width 2 mT, scanning time 20 s/10 mT, time constant 0.1 s, and interval time 10 s between each measurement. Ranges of the external magnetic field were between 35.5 and 45.5 mT in the blood and tail, and between 34.5 and 44.5 mT in the liver and kidney. The central magnetic field was adjusted to coincide with the field of the central signal due to 4-hydroxy-TEMPO. ESR spectral data were collected and analyzed using an ESPRIT ESR Data System (JEOL, Japan), in which the analogue signals, outputted by the ESR spectrometer were converted into a digital signal and then inputted into a memory device. The intensity of the central signal in the triplet ESR spectrum was used for the pharmacokinetic analysis of 4-hydroxy-TEMPO.

#### ***Calibration Lines and Determination of the Concentration of 4-hydroxy-TEMPO by L-band ESR Equipped with Surface-coil-type Resonators***

To determine the *in vivo* spin probe levels in the blood and organs (liver and kidney) of mice, the calibration lines for the spin probe were prepared. The *in vivo* spin probe concentrations were determined as follows: after several concentrations of 4-hydroxy-TEMPO were added to the fresh blood of the untreated mice, 500  $\mu$ l of the solution was transferred to a 600  $\mu$ l volume of a polyethylene tube fixed with SCRs. The intensities of the central signal in the triplet spectrum were monitored. Instrumental conditions were the same as those for *in vivo* measurements, as described. The amounts of 4-hydroxy-TEMPO were obtained from

multiplying its concentrations in a polyethylene tube by the tubular volumes measured with FSCR ( $\pi \times (1.75 \text{ mm})^2 \times 0.32 \text{ mm} = 3.1 \mu\text{l}$ ) and SRSCR ( $\pi \times (3.0 \text{ mm})^2 \times 0.5 \text{ mm} = 14.1 \mu\text{l}$ ) where  $\pi \times (1.75 \text{ mm})^2$  and  $\pi \times (3.0 \text{ mm})^2$  represent the cross section of the cylindrical probe solution for FSCR and SRSCR, respectively, and 0.32 and 0.5 mm, which were measured by a ruler, are the thickness of the solution for FSCR and SRSCR, respectively. ESR signal intensities due to 4-hydroxy-TEMPO obtained from *in vivo* measurements were calibrated to the corresponding spin probe quantities, followed by dividing its quantities by each volume in the blood vessel ( $5 \times 1 \text{ mm}^2 \times 0.32 \text{ mm} = 1.6 \mu\text{l}$ ) and the organ surface ( $\pi \times (5.5 \text{ mm})^2 \times 0.5 \text{ mm} = 47.5 \mu\text{l}$ ) that were actually measured with SCRs, where 5 mm<sup>2</sup> and 0.32 mm are the cross section and thickness of the cubic blood vessel, respectively, and  $\pi \times (5.5 \text{ mm})^2$  and 0.5 mm are those of the cylindrical organ surface, respectively. The *in vivo* concentrations of 4-hydroxy-TEMPO in the blood and organs of mice were, thus, calculated and their disappearances were plotted against the time interval following the administration of 4-hydroxy-TEMPO.

Because the tail of mice is composed of muscle, blood space, nerve and bone, 4-hydroxy-TEMPO in the tail is distributed heterogeneously, which indicates that the quantitative determination of the spin probe is impossible in the tail. Then, we plotted the ESR signal intensities due to 4-hydroxy-TEMPO in the tail against the time interval following the administration of 4-hydroxy-TEMPO.

#### ***Pharmacokinetic Analysis of 4-hydroxy-TEMPO***

The pharmacokinetic parameters for 4-hydroxy-TEMPO were obtained on the basis of a two-compartment model. The equation [ $C = A \exp(-\alpha t) + B \exp(-\beta t)$ ] was fitted to each individual profile of the determined concentrations of 4-hydroxy-TEMPO in the blood, liver and kidney using a nonlinear least squares regression program, MULTI, which was newly rewritten with Visual Basic,<sup>[30]</sup> where  $C$  is the concentration in the blood or tissues,  $\alpha$  and  $\beta$  are the apparent rate constants,  $A$  and  $B$  are the corresponding zero time intercepts and  $t$  is the time. The pharmacokinetic parameters such as area under the concentration curve (AUC), mean residence time (MRT), total body clearance ( $CL_{\text{tot}}$ ), steady-state distribution volume in the body ( $V_{\text{ss}}$ ) and spin clearance rate constant ( $ke$ ) were calculated from the fitted results as follows:  $AUC = A/\alpha + B/\beta$ ,  $MRT = (A/\alpha^2 + B/\beta^2)/(A/\alpha + B/\beta)$ ,  $CL_{\text{tot}} = \text{Dose}/(A/\alpha + B/\beta)$ ,  $V_{\text{ss}} = \text{Dose}(A/\alpha^2 + B/\beta^2)/(A/\alpha + B/\beta)^2$  and  $ke = \alpha\beta(A + B)/(A\beta + \alpha B)$ , respectively, where Dose is the amount of 4-hydroxy-TEMPO administered i.v.<sup>[31,32]</sup>

The spin clearance curves of the signal intensities (s.i.; arbitrary unit) were plotted against time duration following i.v. injection of 4-hydroxy-TEMPO and used for its pharmacokinetic analysis monitored in the tail of mice. The one-compartment model [ $s.i. = A \exp(-ke \times t)$ ] was fitted to these curves by using nonlinear least-squares regression with MULTI to estimate the spin clearance rate constant ( $ke$ ) by curve-fitting.

#### Parameters Derived from the Relationship between the Blood and Organ Data

To examine the relationship of pharmacokinetic parameters in the blood, liver and kidney, which were estimated from the different concentration curves obtained in the local sites of ESR measurement, the secondary pharmacokinetic parameters such as the mean partition coefficient between the blood and organ ( $K_p$ )<sup>[33,34]</sup> and single-pass mean residence time in the organ (MRTSP)<sup>[35–37]</sup> were derived as follows:

$$K_p = AUC_{organ} / AUC_{blood} \quad (1)$$

and

$$MRTSP = MRT_{organ} - MRT_{blood} \quad (2)$$

where the ratio of AUC between the blood and organ ( $K_p$ ) is defined in a non-steady state condition instead of the ratio of concentrations between the blood and organ in a steady-state condition, and the difference in MRT between the blood and organ (MSTSP) quantifying the organ retention property is a function of rate constants associated with efflux and elimination out of the organ and is independent of influx rate constants into the organ from the blood.<sup>[34,36,37]</sup> Using these parameters,  $CL_{tot,organ}$  and  $V_{ss,organ}$  estimated based on the concentration curves in the organ were rearranged to the following

equations:

$$K_p \cdot CL_{tot,organ} = CL_{tot,blood} \quad (3)$$

and

$$\begin{aligned} K_p \cdot V_{ss,organ} &= K_p \cdot CL_{tot,organ} \cdot MRT_{organ} \\ &= V_{ss,blood} + CL_{tot,blood} \cdot MRTSP \quad (4) \end{aligned}$$

In addition,  $CL_{tot,blood} \cdot MRTSP$  ( $\Delta V$ ) was equal to  $CL_{tot,blood} \cdot K_p \cdot V_{organ} / CL_{inf}$ , where  $V_{organ}$  and  $CL_{inf}$  are the actual organ volume and influx clearance into the organ from the blood, respectively.

#### Statistical Analysis

All experimental results were presented as the mean values  $\pm$  standard deviations for 3 or 4 mice. The statistical evaluation was performed by analysis of variance (ANOVA) at a 1 or 5% significant level of difference.

## RESULTS

#### *In Vivo* L-band ESR Measurement using Surface-coil Type Resonators

A triplet L-band ESR signal with equal intensities characteristic of the nitroxide radical was observed in the blood and liver of a mouse that received i.v. injection of 4-hydroxy-TEMPO at a dose of 1.0 mmol/kg body weight, and the disappearance was time-dependent as shown in Fig. 1. Spectra similar to those of the blood and liver were observed in the tail and kidney of a mouse (data not shown). The ESR signal in each organ decreased with time, maintaining its spectral pattern ( $A_N = 1.70$  mT) without the appearance of new signals during measurement.

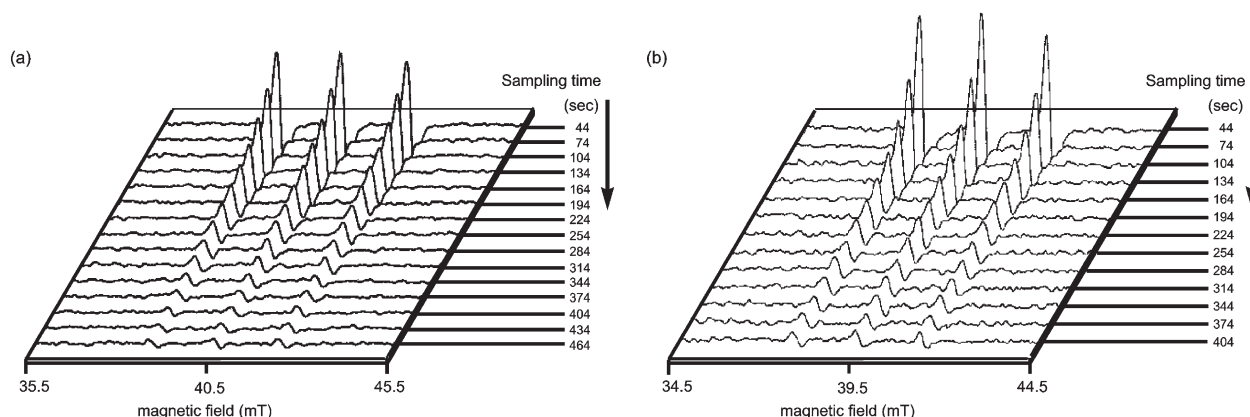


FIGURE 1 Time-dependent ESR spectral changes of 4-hydroxy-TEMPO in (a) the inferior vena cava and (b) the liver of a mouse as monitored by L-band ESR equipped with surface-coil-type resonators at every 30 s.

### Calibration Lines by L-band ESR using Surface-coil Type Resonators

The calibration lines for 4-hydroxy-TEMPO in the fresh blood of mice were obtained by using both (a) FSCR and (b) SRSCR (Fig. 2). Within the sensitivity of the signal intensity due to the spin probe detected by the *in vivo* L-band ESR measurement, the sufficiently correlated calibration lines of 4-hydroxy-TEMPO were obtained by using both (a) FSCR and (b) SRSCR. The detection limits in FSCR and SRSCR were 0.2 and 1.2 nmol at an S/N ratio of 3, and their quantification limits were estimated to be 0.3 and 1.7 nmol at an S/N ratio of 4, respectively. The linear relationships between ESR signal intensities and spin probe quantities were found in the ranges of 0.3–6.2 nmol in FSCR and 1.7–28.3 nmol in SRSCR. The correlation coefficients with linear regression were greater than 0.999 for the four or five concentrations of three repeated measurements in FSCR and greater than 0.997 for the six concentrations of three repeated measurements in SRSCR.

### Quantitative Pharmacokinetic Analysis

ESR signal intensity due to 4-hydroxy-TEMPO was calculated to the corresponding spin-probe quantity based on the calibration lines, and its quantity was divided by the measurement volume in the organs (blood: 1.6  $\mu\text{l}$ , liver and kidney: 47.5  $\mu\text{l}$ ) in order to obtain the concentration of 4-hydroxy-TEMPO in each organ. The time-dependent clearance curves were obtained for the inferior vena cava, liver, and kidney of mice receiving the spin probe at different doses, and they were then changed to the

corresponding time-dependent semi-logarithmic clearance curves as shown in Fig. 3. ESR signals in the liver and kidney of mice given 4-hydroxy-TEMPO at a dose of 0.13 mmol/kg body weight were not detected in a quantitative range. Because each clearance curve showed a two-phase form ( $\alpha$  and  $\beta$ ) in a semi-logarithmic plot (Fig. 3), where the  $\beta$ -phase started about 200 s after injection of 4-hydroxy-TEMPO in the blood and those in the liver and kidney started earlier at approximately 100 s after injection, we analyzed the spin clearance curves on the basis of the two-compartment pharmacokinetic model by using non linear least-squares regression.<sup>[30–32]</sup> The curve fittings to estimate pharmacokinetic parameters were, thus, obtained in the clearance curves in the blood and organs of mice given different doses of the spin probe; the pharmacokinetic parameters such as AUC, MRT,  $CL_{tot}$ ,  $V_{ss}$ , and  $k_e$  in the blood and organs are summarized in Table I. In order to consider the dose-dependent changes of the pharmacokinetic parameters, those in the blood and organs were plotted versus the administered doses as shown in Fig. 4. The AUC in the blood increased dose-independently (3.4–25.2  $\mu\text{mol}\cdot\text{min}/\text{ml}$ ), while the MRT in the blood showed almost constant values (1.8–3.0 min) at all doses (Fig. 4a). No significant dose-dependent changes in  $CL_{tot}$  (30–40 ml/min/kg) and  $V_{ss}$  (70–120 ml/kg) in the blood were observed (Fig. 4b). In regard to the pharmacokinetic parameters in the liver and kidney, the AUC also increased in a dose-dependent manner in the liver, but the AUC in the kidney was saturated at the highest dose (1.0 mmol/kg) (Fig. 4c,d). The MRT (3.2–4.5 min)

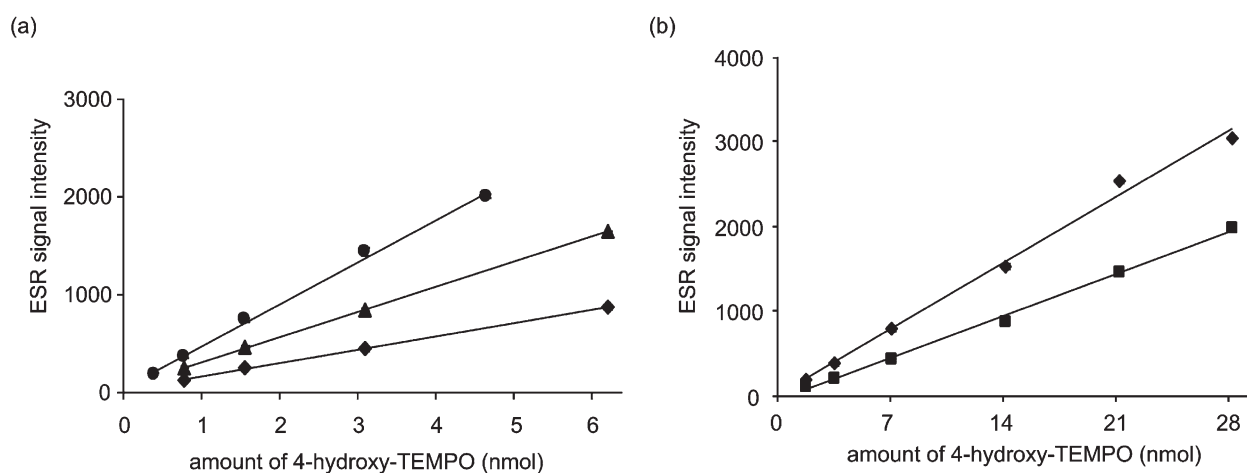


FIGURE 2 Calibration lines of 4-hydroxy-TEMPO dissolved in the fresh blood of untreated mice with a polyethylene tube (600  $\mu\text{l}$ ) measured by L-band ESR using the (a) flexible surface-coil-type and (b) semi-rigid surface-coil-type resonators. The measurement conditions and obtained results were as follows: (a) microwave power; 10 mW ( $\blacklozenge$ ,  $\blacktriangle$ ) or 30 mW ( $\bullet$ ), receiver gain; 250 ( $\blacklozenge$ ) or 500 ( $\blacktriangle$ ,  $\bullet$ ), detection limit (S/N ratio of 3); 0.2 nmol ( $\bullet$ ) or 0.6 nmol ( $\blacklozenge$ ,  $\blacktriangle$ ), quantification limit (S/N ratio of 4); 0.3 nmol ( $\bullet$ ) or 0.8 nmol ( $\blacklozenge$ ,  $\blacktriangle$ ), linearity with  $r > 0.999$  for the four or five concentrations of three repeated measurements; 0.3–4.7 nmol ( $\bullet$ ) or 0.8–6.2 nmol ( $\blacklozenge$ ,  $\blacktriangle$ ). (b) Microwave power; 10 mW, receiver gain; 250 ( $\blacksquare$ ) or 500 ( $\blacklozenge$ ), detection limit (S/N ratio of 3); 1.2 nmol, quantification limit (S/N ratio of 4); 1.7 nmol, linearity with  $r > 0.997$  for the six concentrations of three repeated measurements; 1.7–28.3 nmol.

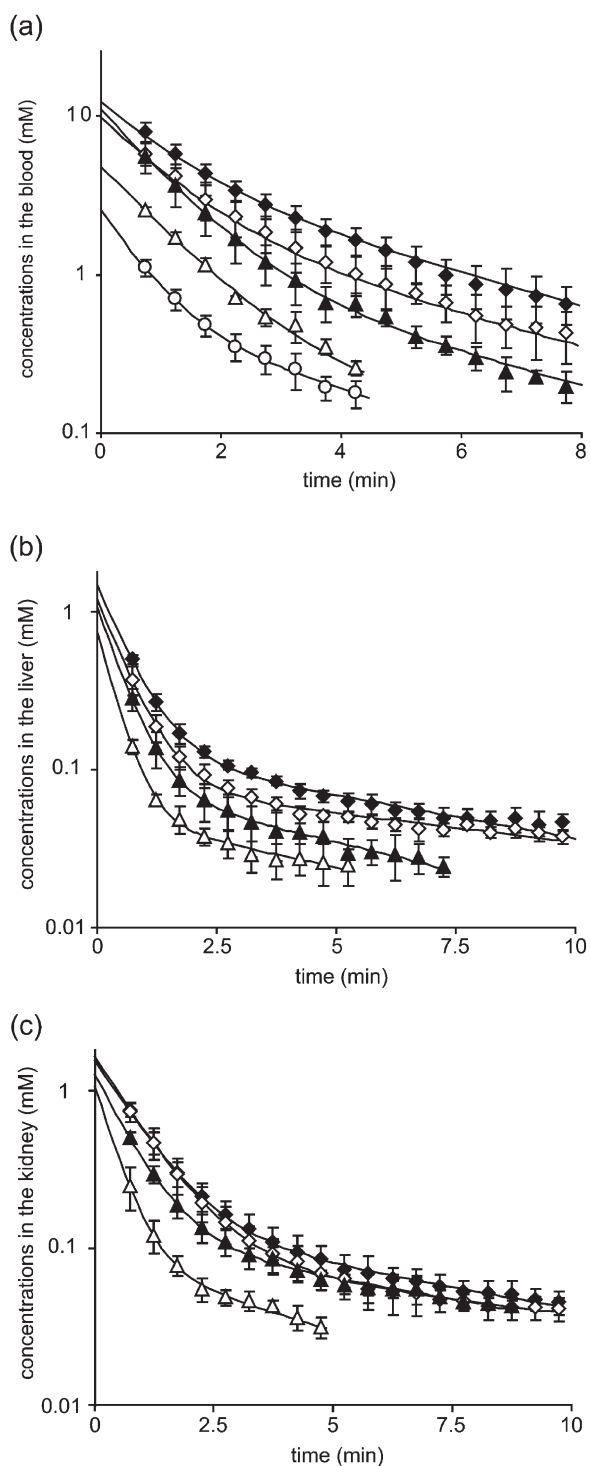


FIGURE 3 Semi-logarithmic clearance curves of the concentrations of 4-hydroxy-TEMPO measured in (a) the inferior vena cava, (b) the liver, and (c) the kidney of mice receiving intravenous injection at doses of 0.13 (○), 0.25 (△), 0.5 (▲), 0.75 (◇), and 1.0 (◆) mmol/kg body weight, respectively. Data and the simulated lines represent the means  $\pm$  standard deviations for 3 or 4 mice and the theoretical curves fitted to the mean value, respectively.

was almost the same in the liver and kidney at all doses (Fig. 4c,d). The significant dose-dependent changes in  $CL_{tot}$  (410–580 and 300–420 ml/min/kg in the liver and kidney, respectively) and  $V_{ss}$

(1600–2400 and 1000–1800 ml/kg in the liver and kidney, respectively) were negligible (Table I).

The time-dependent semi-logarithmic clearance curves were then plotted for the signal intensities in the ESR spectra in the tail of mice receiving the agent at doses of 0.5 and 1.0 mmol/kg body weight (Fig. 5a). Each semi-logarithmic clearance curve showed a linear form different from a two-phased curve measured in the other sites. Therefore, we analyzed the spin clearance curves in the tail on the basis of the one-compartment model by using nonlinear least-squares regression. The  $k_e$  values were estimated to be 0.5–1.0/min, being similar to those in other organs except for the liver, where  $k_e$  decreased in a dose-dependent manner (1.5–0.9/min) (Fig. 5b).

#### Secondary Derived Pharmacokinetic Parameters

In order to compare the pharmacokinetic parameters between the blood and organs, we calculated the secondary parameters derived from Eqs. (1)–(4) in the Experimental section. Secondary pharmacokinetic parameters are summarized in Table II. The partition coefficient ( $K_p$ ) between the blood and organs were estimated to be 0.07–0.1 in the liver/blood and 0.1–0.13 in the kidney/blood, which were almost similar to those at the doses of 0.25–1.0 mmol/kg. Single-pass mean residence times in the organ (MRTSP) were estimated at 1.3–1.9 min in the liver and 1.1–2.3 min in the kidney at doses of 0.25–1.0 mmol/kg, which were shorter compared with the MRT in the blood and organs.  $K_p CL_{tot,organ}$  values in the liver (38–44 ml/min/kg) and kidney (37–44 ml/min/kg) coincided closely with  $CL_{tot,blood}$  (37–40 ml/min/kg) at all doses, while  $K_p V_{ss,organ}$  values in the liver (130–190 ml/kg) and kidney (130–170 ml/kg) showed higher values than  $V_{ss,blood}$  (70–120 ml/kg) because of the apparent additive volume ( $\Delta V$ ).

#### DISCUSSION

ESR spectroscopy has been proposed as a useful tool for detecting and evaluating paramagnetic species in live animals, in which both X- and L-band ESR are used. In the case of X-band ESR, blood circulation monitoring-ESR (BCM-ESR) was proposed in 1997, which realized the real-time spin- and metallo-kinetic analysis in the circulating blood of rats.<sup>[38–41]</sup> While, in case of L-band ESR, both spectroscopy and imaging have been reported for the analysis of spin probes<sup>[8–11]</sup> and nitric oxide (NO)<sup>[42–44]</sup> in mice, being non-quantitative. Then we proposed quantitative *in vivo* L-band ESR spectroscopy for measuring spin probes in mice.<sup>[21]</sup> However, when we understand the kinetics of paramagnetic species in detail,

TABLE I Pharmacokinetic parameters of 4-hydroxy-TEMPO in the blood and organs of mice calculated by the non-linear least squares regression based on the two-compartment model

Domain of measurement	Dose (mmol/kg)	AUC ( $\mu\text{mol}\cdot\text{min}/\text{ml}$ )	MRT (min)	$\text{CL}_{\text{tot}}$ (ml/min/kg)	$V_{\text{ss}}$ (ml/kg)	$k_e$ (1/min)
Blood (inferior vena cava)	0.13	$3.4 \pm 0.4$	$2.9 \pm 0.5$	$37 \pm 5$	$107 \pm 23$	$0.7 \pm 0.1$
	0.25	$6.4 \pm 0.0$	$1.8 \pm 0.3$	$39 \pm 0$	$71 \pm 13$	$0.8 \pm 0.0$
	0.5	$13.5 \pm 0.8$	$2.3 \pm 0.2$	$37 \pm 2$	$85 \pm 13$	$0.8 \pm 0.1$
	0.75	$17.3 \pm 3.2$	$2.8 \pm 0.3$	$30 \pm 5$	$81 \pm 6$	$0.6 \pm 0.1$
	1.0	$25.2 \pm 4.2$	$3.0 \pm 0.7$	$40 \pm 6$	$119 \pm 21$	$0.5 \pm 0.1$
Liver	0.25	$0.6 \pm 0.1$	$3.3 \pm 0.5$	$410 \pm 80$	$1600 \pm 500$	$1.5 \pm 0.4$
	0.5	$1.0 \pm 0.1$	$3.6 \pm 1.0$	$510 \pm 80$	$1800 \pm 500$	$1.2 \pm 0.2$
	0.75	$1.3 \pm 0.2$	$4.2 \pm 0.7$	$580 \pm 70$	$2400 \pm 700$	$1.0 \pm 0.1$
	1.0	$1.8 \pm 0.1$	$4.3 \pm 0.4$	$560 \pm 30$	$2400 \pm 100$	$0.9 \pm 0.1$
Kidney	0.25	$0.9 \pm 0.2$	$3.2 \pm 1.1$	$300 \pm 60$	$1000 \pm 400$	$1.2 \pm 0.2$
	0.5	$1.7 \pm 0.2$	$4.5 \pm 0.3$	$300 \pm 30$	$1400 \pm 200$	$0.7 \pm 0.1$
	0.75	$2.4 \pm 0.4$	$3.8 \pm 0.7$	$330 \pm 60$	$1300 \pm 400$	$0.8 \pm 0.1$
	1.0	$2.4 \pm 0.3$	$4.3 \pm 0.5$	$420 \pm 60$	$1800 \pm 200$	$0.9 \pm 0.1$

Data are expressed as the means  $\pm$  standard deviations for 3 or 4 mice. Significant level: \* $P < 0.05$  and \*\* $P < 0.01$ .

it is essentially important to know the concrete expression of their pharmacokinetics in each organ together with that in the blood. We then used the recently developed surface-coil-type resonators,<sup>[24–29]</sup> which enabled the real-time and local measurement in specific organs such as the inferior vena cava, liver, kidney and tail of minimal invasive mice, and performed the quantitative pharmacokinetic analysis of a spin probe with a short-half life,

4-hydroxy-TEMPO, which was administered to mice.

Although the ESR signal due to 4-hydroxy-TEMPO disappeared with time in the organs of mice receiving i.v. injection of the spin probe, the spectral pattern with three equal signal intensities was recorded throughout the measurements (Fig. 1). When the molecule binds with endogenous biomolecules such as proteins, the 1st and 3rd signals

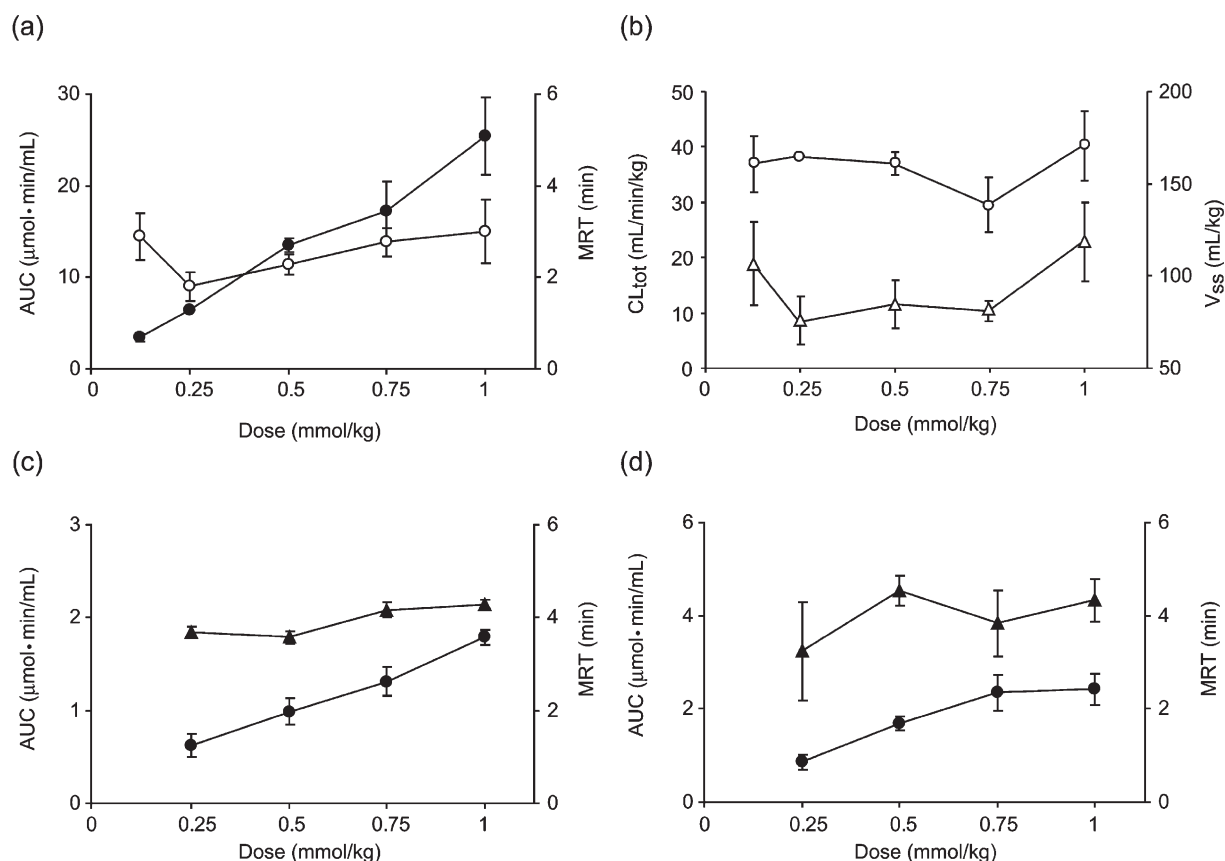


FIGURE 4 Relationships between intravenous doses and pharmacokinetic parameters for 4-hydroxy-TEMPO such as (a) AUC (●) and MRT (▲) in the blood, (b)  $\text{CL}_{\text{tot}}$  (○) and  $V_{\text{ss}}$  (Δ) in the blood, (c) AUC (●) and MRT (▲) in the liver, and (d) AUC (●) and MRT (▲) in the kidney.

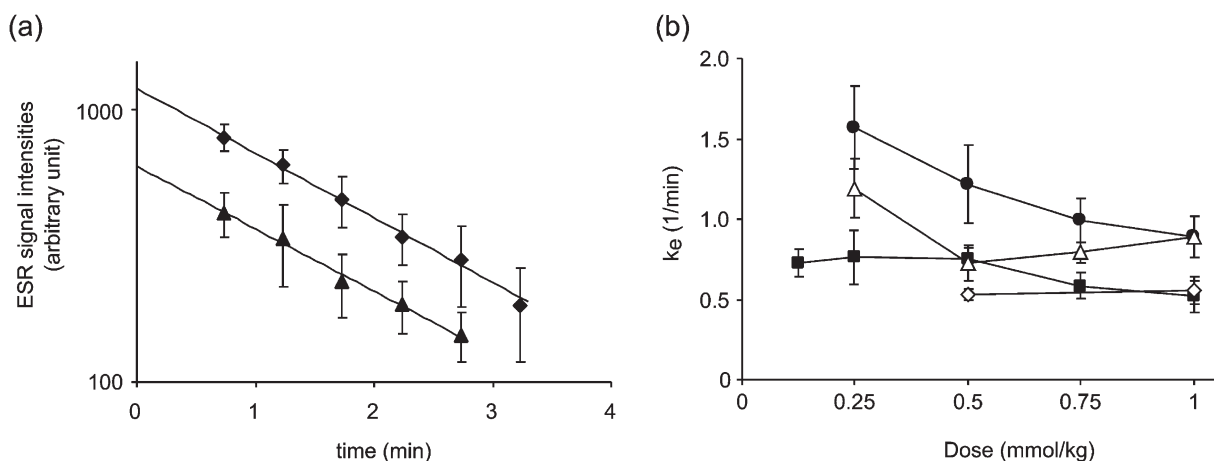


FIGURE 5 (a) Semi-logarithmic clearance curves of the signal intensities due to 4-hydroxy-TEMPO measured in the tail of mice receiving intravenous injection at doses of 0.5 (▲) and 1.0 (◆) mmol/kg body weight. Data and the simulated lines represent the means  $\pm$  standard deviations for 3 mice and the theoretical curves fitted to the mean value, respectively. (b) Relationships between intravenous doses and clearance rate constants for 4-hydroxy-TEMPO estimated from clearance curves in the blood (■), liver (●), kidney ( $\Delta$ ), and tail ( $\diamond$ ) respectively.

become smaller and broader because of the restriction of the thermal molecular movement.<sup>[38,45]</sup> Consequently, most of the observed spin probe was considered to exist as the free form in each mouse organ.

It has been reported from *in vitro* and *in vivo* studies that spin probes administered to animals were reduced to ESR silent hydroxylamines in the blood and cytosols by endogenous reducing agents such as NAD(P)H and ascorbate.<sup>[46–49]</sup> Intravenously injected 4-hydroxy-TEMPO was, thus, indicated to be reduced in the liver and other organs and then excreted into the urine through the kidney,<sup>[21,50]</sup> the amounts of the spin probe and its reduced form excreted into the urine of mice being estimated to be approximately 0.9 and 13% of the dose, respectively, at 2 h after the administration.<sup>[21]</sup> The urinary clearance of the unchanged spin probe was estimated to be less than 1% of the total clearance of 4-hydroxy-TEMPO. In addition, 4-hydroxy-TEMPO was confirmed to be relatively stable in the fresh blood of mice, where its *in vitro*

half-life was estimated to be approximately 35 min by using X- and L-band ESR.<sup>[21,38]</sup> Therefore, the faster paramagnetic loss of 4-hydroxy-TEMPO in the circulating blood (Fig. 1) was thought to be affected by the transport to the tissues, while those in the liver and kidney were presumably caused by the reduction induced by endogenous components in the organs.

Spin clearance curves of the concentration of 4-hydroxy-TEMPO in the blood, liver and kidney (Fig. 3) of mice receiving i.v. injection of 4-hydroxy-TEMPO decreased time-dependently in a two-phase pattern at all doses tested. On the other hand, spin clearance curves detected in the tail disappeared mono-exponentially at the doses of 0.5 and 1.0 mmol/kg body weight (Fig. 5a), probably due to the restricted detection of the spin probe in the blood vessel of the tail. In our previous studies, the concentration of 4-hydroxy-TEMPO monitored by BCM-ESR decreased bi-exponentially in the circulating blood of rats receiving an i.v. dose of 0.01 mmol/kg body weight,<sup>[38]</sup> while the amount of

TABLE II Derived pharmacokinetic parameters of 4-hydroxy-TEMPO from the relationships between the blood and organ data

Domein of measurement	Dose (mmol/kg)	$K_p$	MRTSP (min)	$K_p CL_{tot}$ (ml/min/kg)	$K_p V_{ss}$ (ml/kg)	$\Delta V$ (ml/kg)
Liver	0.25	0.097	1.9	40	150	78
	0.5	0.073	1.3	38	130	49
	0.75	0.073	1.4	44	190	104
	1.0	0.071	1.3	40	170	50
Kidney	0.25	0.134	1.4	40	130	59
	0.5	0.125	2.3	37	170	82
	0.75	0.136	1.1	44	170	92
	1.0	0.095	1.3	40	170	54

Each parameter was calculated as follows:  $K_p = AUC_{organ}/AUC_{blood}$ ,  $MRTSP = MRT_{organ} - MRT_{blood}$ , and  $\Delta V = K_p V_{ss,organ} - V_{ss,blood}$ .



4-hydroxy-TEMPO detected by L-band ESR disappeared in a mono-phase pattern in the head of mice receiving i.v. doses of 0.25–1.0 mmol/kg body weight.<sup>[21]</sup> The difference in spin clearance curves was considered to be due to the detection limit of the radical dependent on the difference in ESR methods.

In the present study, we analyzed the time-dependent biphasic spin clearance curves of 4-hydroxy-TEMPO, where the redistribution of 4-hydroxy-TEMPO from the organs to the blood space was observed in the  $\beta$ -phase of spin clearance curves. When we obtain a more sensitive L-band ESR in the future than the present ESR, we will be able to detect much lower levels of the *in vivo* concentrations of the spin probes.

BCM-ESR in the circulating blood of rats had the highest sensitivity among the *in vivo* ESR methods<sup>[38]</sup> and the present ESR with SCRs was found to be more sensitive in comparison with other conventional L-band ESR equipped with a loop-gap-type resonator monitored at the head or abdomen of mice.<sup>[21]</sup> Because dose-dependent clearance curves for the concentrations of 4-hydroxy-TEMPO were quantitatively obtained in the blood and organs at doses of 0.25–1.0 mmol/kg body weight (Fig. 3), pharmacokinetic analysis based on a two-compartment model was performed in order to evaluate the local disposition of the spin probe (Table I).

As judged by the dose-dependence in the AUC and the dose-independence in MRT,  $CL_{tot}$  and  $V_{ss}$  values (Table I and Fig. 4), 4-hydroxy-TEMPO was considered to exhibit linear disposition in the blood at doses of 0.13–1.0 mmol/kg body weight. Dose-dependence in the AUC in the liver, saturation in the AUC in the kidney and dose-independence in the MRT in both organs (Table I and Fig. 4) indicated the linear distribution of 4-hydroxy-TEMPO in the liver and the slightly saturated distribution of the spin probe in the kidney from the blood compartment. Similar  $k_e$  values of 4-hydroxy-TEMPO in each measurement site (Table I and Fig. 5b) suggested that  $k_e$  could be equivalently estimated independent from the organs of mice.

$CL_{tot}$  and  $V_{ss}$  values in the organs were considerably larger than those in the blood due to the lower concentrations and AUC values in the organs (Fig. 3 and Table I). In order to understand the organ-dependent pharmacokinetic parameters and examine their relationships between the blood and organs in detail, secondary parameters such as  $K_p$  and MRTSP were introduced (Eqs. (1)–(4) and Table II).  $K_p$  values in the liver and kidney were estimated to be approximately 0.08 and 0.12, respectively, showing the low distribution capability into these organs of 4-hydroxy-TEMPO (Table II). 4-Hydroxy-TEMPO was found to distribute to the blood space within several organs such as liver and kidney,<sup>[51]</sup> indicating that the concentration of the spin probe in

the organs was always diminished in comparison with that in the circulating blood vessels. The present results showing the low distribution property of 4-hydroxy-TEMPO in the liver and kidney demonstrate close agreement with the previous finding.<sup>[51]</sup> Then,  $K_p CL_{tot,organ}$  in the liver and kidney were corrected to be approximately 40 ml/min/kg corresponding to  $CL_{tot,blood}$ , while  $K_p V_{ss,organ}$  values were larger than that of  $V_{ss,blood}$  due to  $\Delta V$  (Table II). The additive value,  $\Delta V$ , was produced by an increase of MRT in organs in terms of MRTSP (Eq. (4)). Because MRTSP was a parameter indexing the elimination ability of 4-hydroxy-TEMPO in the organ compartment, such as reduction rate, 4-hydroxy-TEMPO was suggested to be rapidly reduced in the cytosols of the liver and kidney within approximately 1–2 min of the mean residence time (Table II). On the basis of the obtained relationships of the pharmacokinetic parameters between the blood and organ compartments (Eqs. (1)–(4)), describing the spin clearance curves in each organ were systematically interpreted in relation to those in the blood.

## CONCLUSION

The local disposition of 4-hydroxy-TEMPO in the organs of mice was examined by means of the real-time *in vivo* L-band ESR equipped with SCRs, and found to depend on the measurement sites. The dose-dependent clearance curves of 4-hydroxy-TEMPO in the blood, liver, kidney and tail of mice were studied quantitatively using pharmacokinetic model analysis, suggesting the linear distribution and elimination of 4-hydroxy-TEMPO in those organs. *In vivo* L-band ESR with SCRs was, thus, proposed to be a useful method to investigate the local disposition and quantitative pharmacokinetics of paramagnetic species in the organs of animals. The proposed method might provide an effective tool for the detection of endogenously generated free radicals such as reactive oxygen species (ROS)<sup>[52–54]</sup> and nitric oxide (NO),<sup>[42–44]</sup> and for the evaluation of their organ distribution and elimination.

## References

- [1] Halliwell, B. and Gutteridge, J.M.C. (1998) *Free Radicals in Biology and Medicine*, 3rd Ed. (Oxford Science Publications, London).
- [2] Rice-Evans, C.A., Burdorn, R.H., eds, (1994) *Free Radical Damage and its Control* (Elsevier, Amsterdam).
- [3] Saifutdinov, R.G., Larina, L.I., Vakul'skaya, T.I. and Voronkov, M.G. (2001) *Electron Paramagnetic Resonance in Biochemistry and Medicine* (Kluwer Academic/Plenum Publishers, New York).
- [4] Ono, M., Ogata, T., Hsieh, K., Suzuki, M., Yoshida, E. and Kamada, H. (1986) "L-band ESR spectrometer using a loop-gap resonator for *in vivo* analysis", *Chem. Lett.*, 491–494.

- [5] Zweier, J.L. and Kuppusamy, P. (1998) "Electron paramagnetic resonance measurements of free radicals in the intact beating heart: a technique for detection and characterization of free radicals in whole biological tissues", *Proc. Natl Acad. Sci. USA* **85**, 5703–5708.
- [6] Rosen, G.M., Halpern, H.J., Brunsting, L.A., Spencer, D.P., Strauss, K.E., Bowman, M.K. and Wechsler, A.S. (1988) "Direct measurement of nitroxide pharmacokinetics in isolated hearts situated in a low-frequency electron spin resonance spectrometer: implications for spin trapping and *in vivo* oxymetry", *Proc. Natl Acad. Sci. USA* **85**, 7772–7776.
- [7] Hirata, H. and Ono, M. (1996) "Resonance frequency estimation of a bridged loop-gap resonator used for magnetic resonance measurements", *Rev. Sci. Instrum.* **67**, 73–78.
- [8] Berliner, L.J. and Wan, X. (1989) "*In vivo* pharmacokinetics by electron magnetic resonance spectroscopy", *Magn. Reson. Med.* **9**, 430–434.
- [9] Ferrari, M., Colacicchi, S., Gualtieri, G., Santini, M.T. and Sotgiu, A. (1990) "Whole mouse nitroxide free radical pharmacokinetics by low frequency electron paramagnetic resonance", *Biochem. Biophys. Res. Commun.* **166**, 168–173.
- [10] Kuppusamy, P., Chzhnan, M., Vij, K., Shteynbuk, M., Lefler, D.J., Giannella, E. and Zweier, J.L. (1994) "Three-dimensional spectral-spatial EPR imaging of free radicals in the heart: a technique for imaging tissue metabolism", *Proc. Natl Acad. Sci. USA* **91**, 3388–3392.
- [11] Halpern, H.J., Peric, M., Yu, C., Barth, E.D., Chandramouli, G.V.R., Makinen, M.W. and Rosen, G.M. (1996) "*In vivo* spin-label murine pharmacodynamics using low-frequency electron paramagnetic resonance imaging", *Biophys. J.* **71**, 403–409.
- [12] Ishida, S., Matsumoto, S., Yokoyama, H., Mori, N., Kumashiro, H., Tsuchihashi, N., Ogata, T., Yamada, M., Ono, M., Kitajima, T., Kamada, H. and Yoshida, E. (1992) "An ESR-CT imaging of the head of a living rat receiving an administration of a nitroxide radical", *Magn. Reson. Imaging* **10**, 109–114.
- [13] Yokoyama, H., Ogata, T., Tsuchihashi, N., Hiramatsu, M. and Mori, N. (1996) "A spatiotemporal study on the distribution of intraperitoneally injected nitroxide radical in the rat head using an *in vivo* ESR imaging system", *Magn. Reson. Imaging* **14**, 559–563.
- [14] Sano, H., Naruse, M., Matsumoto, K., Oi, T. and Utsumi, H. (2000) "A new nitroxyl-probe with high retention in the brain and its application for brain imaging", *Free Radic. Biol. Med.* **28**, 959–969.
- [15] Yokoyama, H., Itoh, O., Ogata, T., Obara, H., Ohya-Nishiguchi, H. and Kamada, H. (1997) "Temporal brain imaging by a rapid scan ESR-CT system in rats receiving intraperitoneal injection of a methyl ester nitroxide radical", *Magn. Reson. Imaging* **15**, 1079–1084.
- [16] Togashi, H., Shinzawa, H., Ogata, T., Matsuo, T., Ohno, S., Saito, K., Yamada, N., Yokoyama, H., Noda, H., Oikawa, K., Kamada, H. and Takahashi, T. (1998) "Spatiotemporal measurement of free radical elimination in the abdomen using an *in vivo* ESR-CT imaging system", *Free Radic. Biol. Med.* **25**, 1–8.
- [17] Yokoyama, H., Lin, Y., Itoh, O., Ueda, Y., Nakajima, A., Ogata, T., Sato, T., Ohya-Nishiguchi, H. and Kamada, H. (1999) "EPR imaging for *in vivo* analysis of a half-life of a nitroxide radical in the hippocampus and cerebral cortex of rats after epileptic seizures", *Free Radic. Biol. Med.* **27**, 442–448.
- [18] Miura, Y., Anzai, K., Takeshita, S. and Ozawa, T. (1997) "A novel lipophilic spin probe for the measurement of radiation damage in mouse brain using *in vivo* electron spin resonance (ESR)", *FEBS Lett.* **419**, 99–102.
- [19] Phumala, N., Ide, T. and Utsumi, H. (1999) "Noninvasive evaluation of *in vivo* free radical reactions catalyzed by iron using *in vivo* ESR spectroscopy", *Free Radic. Biol. Med.* **26**, 1209–1217.
- [20] Miura, Y., Anzai, K., Ueda, J.I. and Ozawa, T. (2001) "Pathophysiological significance of *in vivo* ESR signal decay in brain damage caused by X-irradiation: radiation effect on nitroxyl decay of a lipophilic spin probe in the head region", *Biochim. Biophys. Acta* **1525**, 167–172.
- [21] Nishino, N., Yasui, H. and Sakurai, H. (1999) "*In vivo* L-band ESR and quantitative pharmacokinetic analysis of stable spin probes in rats and mice", *Free Radic. Res.* **31**, 35–51.
- [22] Quaresima, V., Alecci, M., Ferrari, M. and Sotgiu, A. (1992) "Whole rat electron paramagnetic resonance imaging of a nitroxide free radical by a radio frequency (280 MHz) spectrometer", *Biochem. Biophys. Res. Commun.* **183**, 829–835.
- [23] Alecci, M., Ferrari, M., Quaresima, V., Sotgiu, A. and Ursini, C.L. (1994) "Simultaneous 280 MHz EPR Imaging of rat organs during nitroxide free radical clearance", *Biophys. J.* **67**, 1274–1279.
- [24] Hirata, H., Iwai, H. and Ono, M. (1995) "Analysis of a flexible surface-coil-type resonator for magnetic resonance measurements", *Rev. Sci. Instrum.* **64**, 4529–4534.
- [25] Lin, Y., Yokoyama, H., Ishida, S., Tsuchihashi, N. and Ogata, T. (1997) "*In vivo* spin resonance analysis of nitroxide radicals injected into a rat by a flexible surface-coil-type resonator as an endoscope- or a stethoscope-like device", *Magn. Reson. Mater. Phys. Biol. Med.* **5**, 99–103.
- [26] Honzak, L., Sentjurc, M. and Swartz, H.M. (2000) "*In vivo* EPR of topical delivery of a hydrophilic substance encapsulated in multilamellar liposomes applied to the skin of hairless and normal mice", *J. Control. Release* **66**, 221–228.
- [27] Tada, M., Yokoyama, H., Toyoda, Y., Ohya, H., Ito, T. and Ogata, T. (2000) "Surface-coil-type resonators for *in vivo* temporal ESR measurements in different organs of nitroxide-treated rats", *Appl. Magn. Reson.* **18**, 575–582.
- [28] Yokoyama, H., Tada, M., Sato, T., Ohya, H. and Kamada, H. (2000) "Non-invasive ESR measurements for *in vivo* kinetic studies of a nitroxide radical in the liver of a rat by a surface-coil-type resonator under a field gradient", *Chem. Lett.*, 1000–1001.
- [29] Tada, M., Shiraishi, T., Yokoyama, H., Ohya, H., Ogata, T. and Kamada, H. (2001) "Nondestructive real-time monitoring of the redox status in a potted plant by using a surface-coil-type ESR resonator", *Chem. Lett.*, 1122–1123.
- [30] Yamaoka, K., Tanigawara, Y. and Nakagawa, T. (1981) "A pharmacokinetic analysis program (MULTI) for microcomputer", *J. Pharmacobio-Dyn.* **4**, 879–885.
- [31] Cutler, D.J. (1978) "On the definition of the compartment model concept in pharmacokinetics", *J. Theor. Biol.* **73**, 329–345.
- [32] Gibaldi, M. and Perrier, D. (1982) "Pharmacokinetics", Drug and the Pharmaceutical Sciences, 2nd ed. (Marcel Dekker, New York) **Vol. 15**, pp. 45–109.
- [33] Verotta, D., Sheiner, L.B., Ebling, W.F. and Stanski, D.R. (1989) "A semiparametric approach to physiological flow models", *J. Pharmacokinetic. Biopharm.* **17**, 463–491.
- [34] Björkman, S., Stanski, D.R., Harashima, H., Dowrie, R., Harapat, S.R., Wada, D.R. and Ebling, W.F. (1993) "Tissue distribution of fentanyl and alfentanil in the rat cannot be described by a blood flow limited model", *J. Pharmacokinetic. Biopharm.* **21**, 255–279.
- [35] Lassen, N.A. and Perl, W. (1979) Tracer Kinetic Methods in Medical Physiology (Raven Press, New York), pp. 76–99.
- [36] McNamara, P.J., Fleishaker, J.C. and Hayden, T.L. (1987) "Mean residence time in peripheral tissue", *J. Pharmacokinetic. Biopharm.* **15**, 439–450.
- [37] He, Y.L., Tanigawara, Y., Yasuhara, M. and Hori, R. (1991) "Effect of folic acid on tissue residence and excretion of methotrexate in rats", *Drug Metab. Dispos.* **19**, 729–734.
- [38] Takechi, K., Tamura, H., Yamaoka, K. and Sakurai, H. (1997) "Pharmacokinetic analysis of free radicals by *in vivo* BCM (Blood Circulation Monitoring)-ESR method", *Free Radic. Res.* **26**, 483–496.
- [39] Sakurai, H., Takechi, K., Tsuboi, H. and Yasui, H. (1999) "ESR characterization and metalokinetic analysis of Cr(V) in the blood of rats given carcinogen chromate(VI) compounds", *J. Inorg. Biochem.* **76**, 71–80.
- [40] Yasui, H., Takechi, K. and Sakurai, H. (2000) "Metalokinetic analysis of disposition of vanadyl complexes as insulin-mimetics in rats using BCM-ESR method", *J. Inorg. Biochem.* **78**, 185–196.
- [41] Takino, T., Yasui, H., Yoshitake, A., Hamajima, Y., Matsushita, R., Takada, J. and Sakurai, H. (2001) "A new halogenated antidiabetic vanadyl complex,

- bis(5-iodopicolinato) oxovanadium(IV): *in vitro* and *in vivo* insulinomimetic evaluations and metallokinetic analysis", *J. Biol. Inorg. Chem.* **6**, 133–142.
- [42] Quaresima, V., Takehara, H., Tsushima, K., Ferrari, M. and Utsumi, H. (1996) "*In vivo* detection of mouse liver nitric oxide generation by spin trapping electron paramagnetic resonance spectroscopy", *Biochem. Biophys. Res. Commun.* **221**, 729–734.
- [43] Yoshimura, T., Fujii, H., Takayama, F., Oikawa, K. and Kamada, H. (1996) "*In vivo* EPR detection and imaging of endogenous nitric oxide in lipopolysaccharide-treated mice", *Nat. Biotechnol.* **14**, 992–994.
- [44] Wallis, G., Brackett, D., Lerner, M., Kotake, Y., Bolli, R. and McCay, P.B. (1996) "*In vivo* spin trapping of nitric oxide generated in the small intestine, liver, and kidney during the development of endotoxemia: a time-course study", *Shock* **6**, 274–278.
- [45] Takeshita, K., Utsumi, H. and Hamada, A. (1987) "Dynamic properties of the haptenic site of lipid haptens in phosphatidylcholine membranes. Their relation to the phase transition of the host lattice", *Biophys. J.* **52**, 187–197.
- [46] Vianello, F., Momo, F., Scarpa, M. and Rigo, A. (1995) "Kinetics of nitroxide spin label removal in biological systems: an *in vitro* and *in vivo* ESR study", *Magn. Reson. Imaging* **13**, 219–226.
- [47] Fuchs, J., Groth, N., Herrling, T. and Zimmer, G. (1997) "Electron paramagnetic resonance studies on nitroxide radical 2,2,5,5-tetramethyl-4-piperidin-1-oxyl (TEMPO) redox reactions in human skin", *Free Radic. Biol. Med.* **22**, 967–976.
- [48] Iannone, A., Tomasi, A. and Swartz, H.M. (1990) "Metabolism of nitroxide spin labels in subcellular fraction of rat liver I. Reduction by microsomes", *Biochim. Biophys. Acta* **1034**, 285–289.
- [49] Iannone, A., Tomasi, A., Vannini, V. and Swartz, H.M. (1990) "Metabolism of nitroxide spin labels in subcellular fractions of rat liver. II. Reduction in the cytosol", *Biochim. Biophys. Acta* **1034**, 290–293.
- [50] Matsumoto, S., Mori, N., Tsuchihashi, N., Ogata, T., Lin, Y., Yokoyama, H. and Ishida, S. (1998) "Enhancement of nitroxide-reducing activity in rats after chronic administration of vitamin E, vitamin C, and idebenone examined by an *in vivo* electron spin resonance technique", *Magn. Reson. Med.* **40**, 330–333.
- [51] Togashi, H., Matsuo, T., Shinzawa, H., Takeda, Y., Shao, L., Oikawa, K., Kamada, H. and Takahashi, T. (2000) "*Ex vivo* measurement of tissue distribution of a nitroxide radical after intravenous injection and its *in vivo* imaging using a rapid scan ESR-CT system", *Magn. Reson. Imaging* **18**, 151–156.
- [52] Halpern, H.J., Yu, C., Barth, E., Peric, M. and Rosen, G.M. (1995) "*In situ* detection, by spin trapping, of hydroxyl radical markers produced from ionizing radiation in the tumor of a living mouse", *Proc. Natl Acad. Sci. USA* **92**, 796–800.
- [53] Fink, B., Dikalov, S. and Bassenge, E. (2000) "A new approach for extracellular spin trapping of nitroglycerin-induced superoxide radicals both *in vitro* and *in vivo*", *Free Radic. Biol. Med.* **28**, 121–128.
- [54] Yokoyama, H., Itoh, O., Aoyama, M., Obara, H., Ohya, H. and Kamada, H. (2000) "*In vivo* EPR imaging by using an acyl-protected hydroxylamine to analyze intracerebral oxidative stress in rats after epileptic seizures", *Magn. Reson. Imaging* **18**, 875–879.